Preprints of the
9th International Symposium on Advanced Control of Chemical Processes
The International Federation of Automatic Control
June 7-10, 2015, Whistler, British Columbia, Canada

Distributed Economic Model Predictive Control of a Catalytic Reactor: Evaluation of Sequential and Iterative Architectures

Timothy L. Anderson * **Matthew Ellis** *
Panagiotis D. Christofides *,**,[1]

* *Department of Chemical and Biomolecular Engineering, University of California, Los Angeles, CA, 90095-1592, USA.*
** *Department of Electrical Engineering, University of California, Los Angeles, CA, 90095-1592, USA.*

Abstract: The development and application of distributed economic model predictive control (DEMPC) methodologies to a catalytic reactor is considered. Two DEMPC methodologies are designed for sequential and iterative implementation, respectively. The DEMPC architectures are evaluated on the basis of the closed-loop performance and on-line computation time requirements compared to a centralized EMPC approach. For the catalytic reactor considered, DEMPC proves to be a viable option as it is able to give similar closed-loop performance while reducing the on-line computation time requirements relative to a centralized EMPC strategy.

Keywords: Economic model predictive control, distributed model predictive control, process control, nonlinear systems

1. INTRODUCTION

Operating chemical processes in an economically-optimal manner while maintaining closed-loop stability and satisfying the process constraints is an important issue within chemical process control. To accomplish this objective, model predictive control (MPC) has proven to be an attractive way in many industrial applications (e.g., Qin and Badgwell (2003)). MPC is a control methodology that accounts for performance criterion by optimizing a cost function over a finite-time prediction horizon subject to a process model (to predict the future behavior of the process), process constraints, and stability constraints. Traditionally, the cost function used within MPC is a quadratic cost that is positive definite with respect to an operating steady-state of a process.

Given that MPC is implemented in a receding horizon fashion (i.e., an optimization problem is solved on-line at each sampling time to compute the control actions), significant computation delay may result when computing control actions for process systems of high dimension (i.e., many states and inputs) which may affect closed-loop stability and performance. In the context of control of large-scale nonlinear chemical process networks, an alternative is to employ a distributed MPC (DMPC) architecture (e.g., Christofides et al. (2013)). DMPC has the ability to control large-scale multiple-input multiple-output with input and state constraints while remaining computationally feasible to be implemented on-line through a distributed implementation of the computations. Numerous formulations, implementation strategies, and theoretical results have been developed within the context of standard tracking DMPC (e.g, Liu et al. (2009, 2010); see, also, the reviews of Scattolini (2009); Christofides et al. (2013) and the references therein).

To integrate process (dynamic) optimization and control, economic MPC (EMPC), which optimizes a general cost function that represents the process economics instead of a quadratic cost function, has been proposed as a control methodology that may help to enable future manufacturing tasks like demand-driven process operations (e.g., Huang et al. (2011); Angeli et al. (2012); Heidarinejad et al. (2012); see, also, the review Ellis et al. (2014) and the references therein). Recently, significant effort within the control community has focused on (centralized) EMPC. Since EMPC may use a general (nonlinear) economic cost function and may dictate a time-varying operation strategy, the on-line computation required to solve EMPC may be significant especially for large-scale process networks. Thus, distributed EMPC (DEMPC) may be one choice to significantly reduce the on-line computational burden. To date, only a limited amount of work on DEMPC for linear systems [Driessen et al. (2012); Müller and Allgöwer (2014)] and for nonlinear systems [Chen et al. (2012); Lee and Angeli (2012)] has been completed. While these works on distributed EMPC (DEMPC) have shown some promising results on DEMPC, more work in this direction is in order.

In the present work, sequential and iterative distributed EMPC strategies are developed and applied to a benchmark catalytic reactor where time-varying operation of the reactor gives greater yield of the product compared to steady-state operation. A description of the DEMPC

[1] Corresponding author: Panagiotis D. Christofides. Tel.:+1 310 794 1015; fax: +1 310 206 4107; e-mail: pdc@seas.ucla.edu. Financial support from the National Science Foundation and the Department of Energy is gratefully acknowledged.

implementation strategies is provided. Several closed-loop simulations are performed to evaluate the approaches. Two key performance metrics are considered in the evaluation: the closed-loop economic performance under the various DEMPC strategies and the on-line computation time required to solve the EMPC optimization problems.

1.1 Class of Nonlinear Systems

The class of nonlinear systems considered are described by the following system of first-order ordinary differential equations:

$$\dot{x}(t) = f(x(t), u_1(t), \ldots, u_m(t), w(t)) \tag{1}$$

where $x(t) \in R^{n_x}$ denotes the state vector, $u_i(t) \in R^{n_{u_i}}$ for $i = 1, \ \ldots, \ m$ denotes the ith manipulated (control) input vector, $w(t) \in R^{n_w}$ denotes the disturbance vector. The (full) input vector has been divided into m input vectors given that m distributed controllers will be designed to control each of the m input vectors. The input vectors are bounded in a convex set denoted as $U_i := \{u_i \in R^{n_{u_i}} \mid u_{ij,\min} \leq u_{ij} \leq u_{ij,\max}, \ j = 1, \ \ldots, n_{u_i}\}$ for $i = 1, \ \ldots, \ m$ where $u_{ij,\min}$ and $u_{ij,\max}$ denote the minimum and maximum bound on the jth element of the ith input vector, respectively. Additionally, the disturbance vector is assumed to be bounded: $w(t) \in W := \{w \in R^l \mid |w| \leq \theta\}$ where $\theta > 0$ bounds the norm of the disturbance vector. The vector field of the system of Eq. 1 is assumed to be a locally Lipschitz vector function of its arguments, and the origin of the unforced system is the equilibrium point of Eq. 1 (i.e., $f(0, 0, \ldots, 0, 0) = 0$). A state measurement of the system of Eq. 1 is assumed to be available synchronously at sampling instances denoted as $t_k := t_0 + k\Delta$ where t_0 is the initial time, $k \in I_{\geq 0}$ and $\Delta > 0$ is the sampling period.

1.2 Economic Model Predictive Control

In a centralized approach, one can design an EMPC system that computes control actions for all m input vectors. EMPC, implemented in a centralized approach for the system of Eq. 1, is formulated as follows:

$$\underset{u_1,\ldots,u_m \in S(\Delta)}{\text{maximize}} \quad \int_0^{N\Delta} l_e(\tilde{x}(\tau), u_1(\tau), \ldots, u_m(\tau)) \, d\tau \tag{2a}$$

$$\text{subject to} \quad \dot{\tilde{x}}(\tau) = f(\tilde{x}(\tau), u_1(\tau), \ldots, u_m(\tau), 0) \tag{2b}$$

$$\tilde{x}(0) = x(t_k) \tag{2c}$$

$$u_i(\tau) \in U_i, \ \forall \ \tau \in [0, N\Delta) \tag{2d}$$

$$\int_0^{N\Delta} g(\tilde{x}(\tau), u(\tau)) \, d\tau \leq 0 \tag{2e}$$

where $i = 1, \ldots, m$ and the notation $S(\Delta)$ denotes the family of piecewise constant functions with period Δ, $\tilde{x}(\tau)$ denotes the predicted state trajectory under the piecewise constant input profiles, $u_1(\tau), \ \ldots, \ u_m(\tau)$, which are the decision variable of the dynamic optimization problem, Δ is the sampling period of the EMPC, and N is a positive integer that denotes the prediction horizon (i.e., number of sampling periods in the prediction horizon). To distinguish between real-time and the prediction time of the EMPC, t denotes the real (continuous) time, t_k denotes the discrete sampling instances where state feedback is obtained, and $\tau \in [0, N\Delta)$ denotes the predicted time in the controller.

The stage cost $l_e(x, u_1, \ldots, u_m)$ of the EMPC is one of the design/tuning elements of the EMPC. It is chosen to reflect the process economics and need not be a quadratic stage cost like that typically used with standard tracking MPC. The stage cost of the EMPC is referred to as the economic cost function. The computed input profile optimizes the economic cost (2a) over the prediction horizon while accounting for the following constraints. The constraint (2b) is the dynamic model of the process initialized with a state measurement (2c) received at sampling instance t_k. The nominal dynamic model predicts the future behavior of the process under any input trajectories $u_1(\tau), \ \ldots, u_m(\tau)$ for $\tau \in [0, N\Delta)$ and allows for the EMPC to compute the optimal input trajectories. The optimal input trajectories are denoted: $u_1^*(\tau|t_k), \ \ldots, u_m^*(\tau|t_k)$ for $\tau \in [0, N\Delta)$. The bounds on the inputs are given by the constraints of (2d). Lastly, the constraint (2e) represents economics-based constraints which are typically integral constraints.

EMPC, like standard tracking MPC, is implemented in a receding horizon fashion. At a sampling instance t_k, the controller receives the current state measurement $x(t_k)$, computes the optimal input trajectories $u_1^*(\tau|t_k), \ \ldots, u_m(\tau|t_k)$ for $\tau \in [0, N\Delta)$ (which corresponds from t_k to t_{k+N}), and implements the control action computed for the first sampling period in the prediction horizon on the process: $u_i(t) = u_i^*(0|t_k)$ for $t \in [t_k, t_{k+1})$. The process is repeated at the next sampling time by rolling the horizon one sampling period.

2. CATALYTIC REACTOR EXAMPLE

A catalytic reactor example is considered to evaluate various DEMPC implementation strategies. A non-isothermal continuous stirred tank reactor (CSTR) where ethylene is catalytically converted to ethylene oxide is considered. Besides the oxidation reaction, two combustion reactions occur that consume ethylene and ethylene oxide. The three reactions are given by:

$$\mathrm{C_2H_4} + \frac{1}{2}\mathrm{O_2} \xrightarrow{r_1} \mathrm{C_2H_4O} \tag{R1}$$

$$\mathrm{C_2H_4} + 3\mathrm{O_2} \xrightarrow{r_2} 2\mathrm{CO_2} + 2\mathrm{H_2O} \tag{R2}$$

$$\mathrm{C_2H_4O} + \frac{5}{2}\mathrm{O_2} \xrightarrow{r_3} 2\mathrm{CO_2} + 2\mathrm{H_2O} \tag{R3}$$

The reactor has a cooling jacket to remove the heat generated by the three exothermic reactions. The catalytic reactor has three manipulated inputs: the volumetric flow rate of the reactor feed, the ethylene concentration in the reactor feed, and the coolant jacket temperature.

The gaseous mixture contained in the reactor is assumed to be an ideal gas. By employing other standard modeling assumptions, a dynamic model can be developed for the catalytic reactor, and the resulting dynamic model has four states: the reactor gas mixture density, the reactor ethylene concentration, the reactor ethylene oxide concentration, and the reactor temperature. The states are denoted as x_1, x_2, x_3, and x_4, respectively, and the inputs are denoted u_1, u_2, and u_3, respectively (dimensionless variable form is used for all variables). The complete model can be found in Özgülşen et al. (1992) which uses the nonlinear Arrhenius reaction rate laws of Alfani and Carberry (1970). The admissible input values are given by the following sets:

$$u_1 \in U_1 := [0.0704, 0.7042] \ ,$$
$$u_2 \in U_2 := [0.2465, 2.4648] \ ,$$
$$u_3 \in U_3 := [0.6, 1.1] \ .$$

The economic performance is characterized by the average yield of ethylene oxide which is given by:

$$Y(t_f) = \frac{\int_0^{t_f} u_1(t)x_4(t)x_3(t) \ dt}{\int_0^{t_f} u_1(t)u_2(t) \ dt} \tag{3}$$

where t_f is the length of operation of the catalytic reactor ($t = 0$ is taken to be the initial time of operation). The average molar flow rate of ethylene that may be fed to the reactor is fixed owing to practical considerations:

$$\frac{1}{t_f}\int_0^{t_f} u_1(t)u_2(t) \ dt = 0.175 \ . \tag{4}$$

The economic cost used within EMPC is:

$$l_e(x, u) = u_1 x_4 x_3 \tag{5}$$

which only consists of the numerator of the yield (3) given that the denominator is fixed by the constraint (4). The steady-state $x_s^T = [0.998 \ \ 0.424 \ \ 0.032 \ \ 1.002]$ corresponding to a steady-state input of $u_s^T = [0.35 \ \ 0.5 \ \ 1.0]$ is within the range of operation of interest, satisfies constraint (4), and is open-loop asymptotically stable (i.e., stability is not an issue within the range of operation and the objective of applying EMPC is used to optimize the average yield). In all the simulations below, the process was initialized at the initial condition:

$$x_0^T = [0.95 \ \ 0.50 \ \ 0.21 \ \ 1.00]$$

3. EVALUATION OF DEMPC METHODS TO THE CATALYTIC REACTOR

Several implementation strategies (centralized and distributed) are applied to the catalytic reactor. Studying the benefits of applying EMPC to the catalytic reactor has already been considered. In Ellis and Christofides (2014), improved average yield of ethylene oxide resulted by applying EMPC to the process compared to operating the reactor at steady-state as well as operating the reactor with an open-loop optimal periodic switching of the inputs u_1 and u_2 considered in Özgülşen et al. (1992). The closed-loop simulations below were programmed using C++ on a desktop computer with an Ubuntu Linux operating system and an Intel® Core™ i7 3.4 GHz processor. To recursively solve the catalytic reactor dynamic model, the explicit Euler method was used. A step size of 0.00001 was used to simulate the closed-loop dynamics of the reactor, while a step size of 0.005 was used to solve the model within the EMPC problem; both led to stable numerical integration.

Regarding the implementation details of the EMPC systems below, a sampling period of $\Delta = 1.0$ was used. The optimization problems were solved using the interior point solver Ipopt (Wächter and Biegler (2006)). To account for real-time computation considerations, the solver was forced to terminate after 100 iterations and/or after 100 seconds of computation time. The tolerance of the solver was set to 10^{-5}. To satisfy the constraint on the amount of ethylene that may be fed to the reactor, this constraint was enforced over operating windows of length $t_p = 47$, that is the average molar flow rate of ethylene must be equal to 0.175 at the end of each operating window. A shrinking

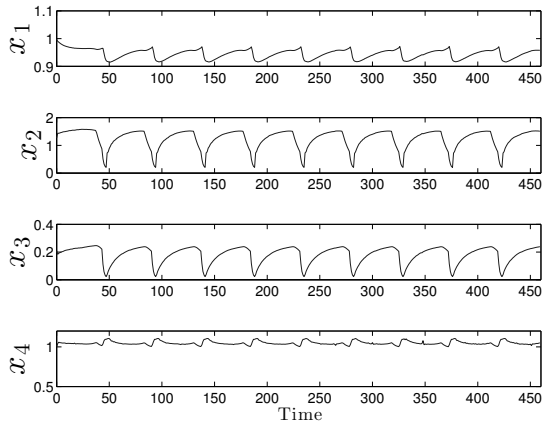

Fig. 1. State trajectories under C-EMPC.

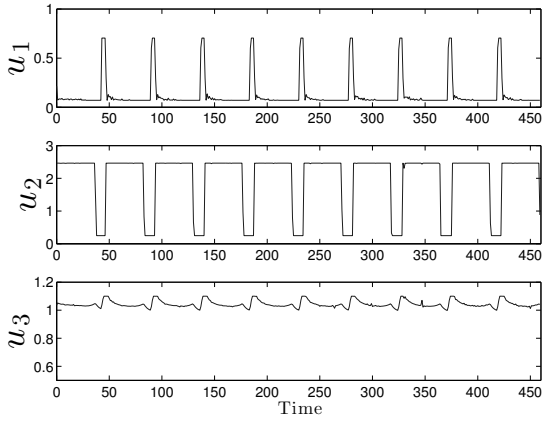

Fig. 2. Input trajectories computed by the C-EMPC.

horizon approach was used within EMPC: at the beginning of the jth operating window, the prediction horizon was set to $N_k := t_p/\Delta$ and the horizon was decreased by one at every subsequent sampling time ($N_k = N_{k-1} - 1$ at the sampling instance t_k). At the beginning of the $(j+1)$th operating window, the prediction horizon was set to t_p/Δ.

3.1 Centralized EMPC

For this computational study, a centralized EMPC strategy, which is denoted C-EMPC, was considered to compare the two distributed implementation strategies and an EMPC of the form (6) was formulated for the catalytic reactor. The C-EMPC formulation is given by:

$$\underset{u_1,u_2,u_3 \in S(\Delta)}{\text{maximize}} \ \int_0^{N_k\Delta} u_1(\tau)\tilde{x}_4(\tau)\tilde{x}_3(\tau) \ d\tau \tag{6a}$$

$$\text{subject to} \ \ \dot{\tilde{x}}(\tau) = f(\tilde{x}(\tau), u_1(\tau), u_2(\tau), u_3(\tau)) \tag{6b}$$

$$u_i(\tau) \in U_i \ \forall \ \tau \in [0, N_k\Delta) \tag{6c}$$

$$\frac{1}{t_p}\int_0^{N_k\Delta} u_1(\tau)u_2(\tau) \ d\tau = 0.175 - \frac{1}{t_p}\int_{t_0+jt_p}^{t_k} u_1^*(t)u_2^*(t) \ dt \tag{6d}$$

where $i = 1, \ 2, \ 3$ and u_1^* and u_2^* denote the optimal control actions applied to the reactor from the beginning of the current operating window to current sampling time, t_k.

Figs. 1-2 depict the closed-loop state and input trajectories under the C-EMPC scheme over ten operating windows. Similar to the results of Ellis and Christofides (2014), the

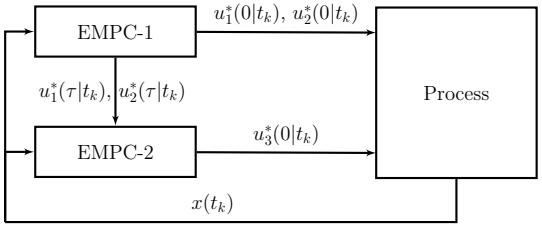

Fig. 3. A block diagram of the S-DEMPC 1-2 scheme.

C-EMPC distributes the ethylene in a non-uniform fashion with respect to time to optimize the yield of ethylene oxide. The average yield of ethylene oxide of the reactor under the C-EMPC is 10.22%. On the other hand, the average yield of ethylene oxide of the reactor over the same length of operation under constant steady-state input values is 6.38%, and the average yield under EMPC is 60% better than that of steady-state operation.

3.2 Sequential DEMPC

A sequential implementation strategy computes the control actions for the process by computing a series of distributed controllers in succession. The first controller computes an input trajectory for the first input trajectory (i.e., u_1 of system (1)). The input trajectory $u_1(t)$ is sent to the next controller to solve for the input trajectory $u_2(t)$. The input trajectory $u_3(t)$ is computed by the third controller after the input trajectories $u_1(t)$ and $u_2(t)$ are received from the previous controllers. The process is repeated until control actions for all m input vectors have been computed.

For this process example, which has three inputs, a reasonable choice of input grouping can be made as a consequence of the integral input constraint (4) (i.e., u_1 and u_2 should be computed by the same EMPC, while it is worth investigating if the input u_3 can be placed on another EMPC system). This input pairing will be used in all of the DEMPC schemes below and the resulting EMPC system that computes control actions for u_1 and u_2 is denoted as EMPC-1, and the other EMPC that computes control actions for u_3 is denoted as EMPC-2. The formulations of each EMPC system follows from the centralized EMPC formulation (6) and are omitted due to space constraints.

Sequential DEMPC 1-2 The first configuration considered, which is referred to as the sequential DEMPC 1-2 (abbreviated as S-DEMPC 1-2), first computes EMPC-1 for the optimal input trajectories $u_1^*(\tau|t_k)$ and $u_2^*(\tau|t_k)$ for $\tau \in [0, N_k\Delta)$. Then, EMPC-2 computes the input trajectory $u_3^*(\tau|t_k)$ after receiving $u_1^*(\tau|t_k)$ and $u_2^*(\tau|t_k)$ from EMPC-1. Since the input trajectory $u_3(\tau)$ has not been determined when EMPC-1 is computed, it is set to be the resulting input trajectory under a PI controller implemented in a sample-and-hold fashion over the prediction horizon (other methods for the assumed profile of $u_3(t)$ within EMPC-1 could be considered). The input constraints are accounted for in the computed PI input trajectory (e.g., if the PI controller computed a control action greater than the upper bound on u_3, it was set to $u_{3,\max}$). The optimal input trajectories $u_1^*(\tau|t_k)$ and $u_2^*(\tau|t_k)$ are used in EMPC-2 to predict the behavior of the reactor over the prediction horizon (i.e., the optimization problem of EMPC-2 is similar to (6) except the decision variable is u_3 only, $u_1(\tau)$ and $u_2(\tau)$ are set to the values computed by EMPC-1, and there is no integral input constraint (6d)). A block diagram of the resulting control architecture is given in Fig. 3.

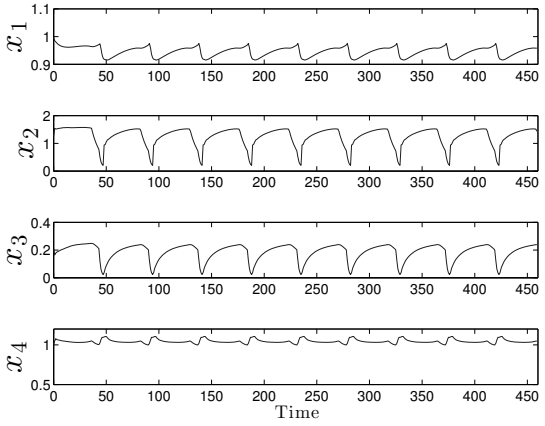

Fig. 4. State trajectories under the S-DEMPC 1-2.

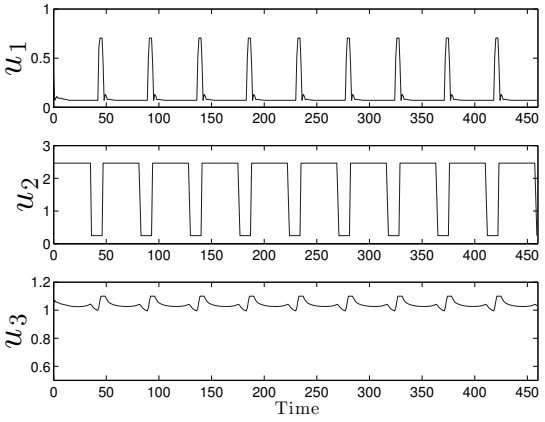

Fig. 5. Input trajectories computed by the S-DEMPC 1-2.

Figs. 4-5 show the closed-loop state and input trajectories under the S-DEMPC 1-2, respectively, and the trajectories are similar to those under the C-EMPC (Figs. 1-2). For this closed-loop simulation, the average yield was 10.20% (recall, the average yield under the C-EMPC was 10.22%). The difference between the average yield under the C-EMPC and under the S-DEMPC 1-2 is small and likely numerically insignificant given the solver parameters used. Some differences in the state trajectories are observed from Fig. 1 and Fig. 4 (e.g., $x_1(t)$ and $x_4(t)$). It is important to note that given the nonlinear nature of the process considered, there is no guarantee, in general, that the centralized EMPC and sequential EMPC scheme will lead to the same optimal input trajectories.

Sequential DEMPC 2-1 Another sequential implementation of EMPC-1 and EMPC-2 may be considered by reversing the execution of EMPC-1 and EMPC-2. In this case, EMPC-2 computes its optimal input trajectory $u_3^*(\tau|t_k)$ first. The sequential DEMPC approach is referred to as sequential DEMPC 2-1 (S-DEMPC 2-1). To solve EMPC-2, the trajectories $u_1(\tau)$ and $u_2(\tau)$ are set to the input trajectories resulting from two PI controllers implemented in sample-and-hold fashion. While the bounds on admissible input values are accounted for in the PI input trajectories, the input average constraint of Eq. 4 is

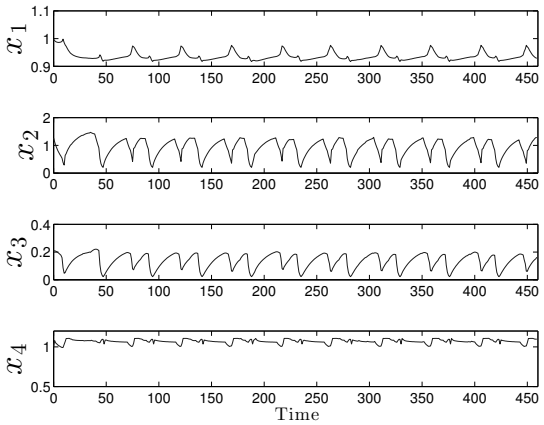

Fig. 6. State trajectories under the S-DEMPC 2-1.

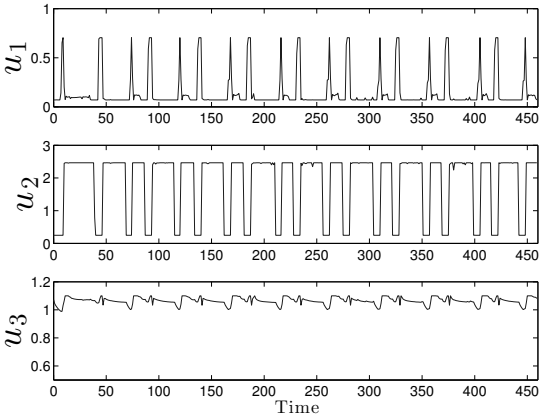

Fig. 7. Input trajectories of computed by the S-DEMPC 2-1.

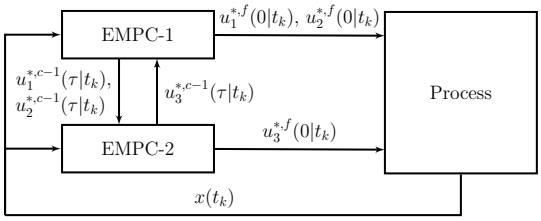

Fig. 8. A block diagram of the I-DEMPC scheme.

not accounted for in the PI input trajectories. The block diagram describing this DEMPC architecture is similar to that of Fig. 3 with communication between EMPC-1 and EMPC-2 in the opposite direction. Figs. 6-7 are the closed-loop state and input trajectories under the S-DEMPC 2-1 approach. Compared to the other trajectories more noticeable differences are observed.

3.3 Iterative DEMPC

Instead of sequential computation of the distributed EMPC schemes, parallel computation may be employed. Given the control actions are computed without the knowledge of the control actions computed by the other distributed EMPC schemes, an iterative approach may be used to (ideally) compute control actions closer to the centralized solution. It is important to note that given the nonlinearity and non-convexity of the optimization problems, it is difficult, in general, to guarantee that an iterative DEMPC strategy will converge to the centralized

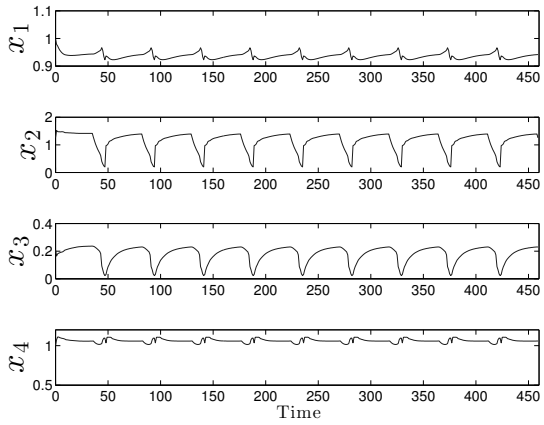

Fig. 9. State trajectories under the I-DEMPC (1 iteration).

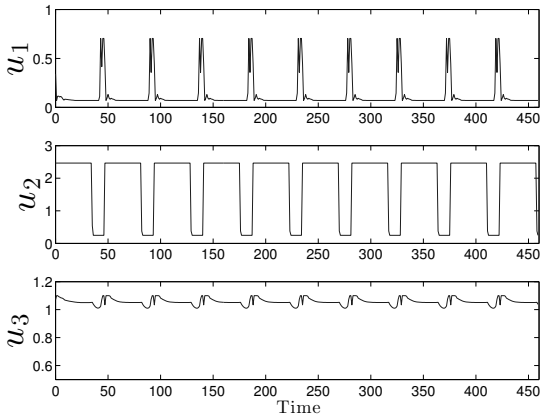

Fig. 10. Input trajectories of computed by the I-DEMPC (1 iteration).

solution (even after infinite iterations). Moreover, there is no guarantee that the input solution computed at each iteration improves upon the closed-loop performance over the previous iteration. An iterative DEMPC (I-DEMPC) scheme is designed for the catalytic reactor and a block diagram of the I-DEMPC control architecture is given in Fig. 8. The computed input trajectories at each iteration of the I-DEMPC is denoted as $u_i^{*,c}(\tau|t_k)$, $i = 1, 2, 3$ where c is the iteration number. At the first iteration, the input trajectory u_3 in EMPC-1 is initialized with the sample-and-hold input trajectory computed from the same PI controller used in the S-DEMPC 1-2 scheme, and similarly, the input trajectories u_2 and u_3 for EMPC-2 are computed from the PI controllers of the S-DEMPC 2-1 scheme. The control action applied to the reactor is denoted as $u_i^{*,f}(t_k|t_k)$ for $i = 1, 2, 3$ where f is the number of iterations of the iterative DEMPC scheme (f is a design parameter of the scheme). When $f = 1$, the I-EMPC scheme is decentralized in the sense that there is no communication between EMPC-1 and EMPC-2.

For this example, no closed-loop performance benefit was observed after iterating more than once through the I-DEMPC scheme. In fact, using the previous iterate solution to compute the next iterative gave worse closed-loop performance than applying the first computed iteration to the process. One method considered to compensate for this problem was to use the best computed input solution over all iterations to compute the next iteration. However, minimal closed-loop performance benefit was

Table 1. The average yield and computation time under the EMPC strategies.

Strategy	Yield (%)	Comp. time (s)
Sequential DEMPC 1-2	10.20	1.039
Sequential DEMPC 2-1	9.92	2.969
Iterative DEMPC ($f = 1$)	10.05	0.832
Centralized EMPC	10.22	4.244

observed with this method as well. Thus, $f = 1$ for this case given that using more than one iteration did not improve the closed-loop performance. The resulting closed-loop trajectories are given in Figs. 9-10. The trajectories have similar characteristics as the centralized case.

3.4 Evaluation of DEMPC Approaches

The average yield and average computation time required to solve the optimization problem at each sampling time over the entire simulation were considered for all the cases. The sequential DEMPC computation time is computed as the sum of the computation time of EMPC-1 and EMPC-2 at each sampling time because the sequential DEMPC schemes are computed sequentially. The iterative DEMPC is computed as the maximum computation time of any one EMPC at each sampling time (recall only one iteration was used). The average yield and average computation time for all the cases is given in Table 1. The centralized EMPC, sequential DEMPC 1-2, and iterative DEMPC schemes all gave similar closed-loop performance. The sequential DEMPC 1-2 and iterative DEMPC result in approximately a 70% reduction in computation time over the centralized EMPC. The sequential DEMPC 2-1 scheme not only had the worst performance of all the strategies considered (albeit still better than steady-state operation), but also, required a comparable amount of time to solve the optimization problems as the centralized case, thereby implying a strong dependence of closed-loop performance on controller calculation sequence. DEMPC was able to yield comparable closed-loop performance while substantially reducing the on-line computation time. This demonstrates that a distributed implementation may allow EMPC to be used on processes where centralized control is not feasible due to the solve time.

This example illustrates another key point within the context of DEMPC. Specifically, the inclusion of integral constraint in EMPC may be an important consideration for input selection in DEMPC. From the sequential DEMPC results, the computed u_3 profile is impacted by the assumed input profiles u_1 and u_2 (Fig. 7), while u_1 and u_2 are not affected as much by the assumed profile u_3 (Fig. 5) compared to the centralized EMPC case (Fig. 2). This behavior may be due to the enforcement of the integral input constraint, and for this example, there may only be one method to distribute a fixed amount of ethylene to the reactor that maximizes the yield that is independent of u_3.

REFERENCES

Alfani, F. and Carberry, J.J. (1970). An exploratory kinetic study of ethylene oxidation over an unmoderated supported silver catalyst. *La Chimica e L'Industria*, 52, 1192–1196.

Angeli, D., Amrit, R., and Rawlings, J.B. (2012). On average performance and stability of economic model predictive control. *IEEE Transactions on Automatic Control*, 57, 1615–1626.

Chen, X., Heidarinejad, M., Liu, J., and Christofides, P.D. (2012). Distributed economic MPC: Application to a nonlinear chemical process network. *Journal of Process Control*, 22, 689–699.

Christofides, P.D., Scattolini, R., Muñoz de la Peña, D., and Liu, J. (2013). Distributed model predictive control: A tutorial review and future research directions. *Computers & Chemical Engineering*, 51, 21–41.

Driessen, P.A.A., Hermans, R.M., and van den Bosch, P.P.J. (2012). Distributed economic model predictive control of networks in competitive environments. In *Proceedings of the IEEE 51st Annual Conference on Decision and Control*, 266–271. Maui, HI.

Ellis, M. and Christofides, P.D. (2014). Optimal time-varying operation of nonlinear process systems with economic model predictive control. *Industrial & Engineering Chemistry Research*, 53, 4991–5001.

Ellis, M., Durand, H., and Christofides, P.D. (2014). A tutorial review of economic model predictive control methods. *Journal of Process Control*, 24, 1156–1178.

Heidarinejad, M., Liu, J., and Christofides, P.D. (2012). Economic model predictive control of nonlinear process systems using Lyapunov techniques. *AIChE Journal*, 58, 855–870.

Huang, R., Harinath, E., and Biegler, L.T. (2011). Lyapunov stability of economically oriented NMPC for cyclic processes. *Journal of Process Control*, 21, 501–509.

Lee, J. and Angeli, D. (2012). Distributed cooperative nonlinear economic MPC. In *Proceedings of the 20th International Symposium on Mathematical Theory of Networks and Systems*. Melbourne, Australia.

Liu, J., Chen, X., Muñoz de la Peña, D., and Christofides, P.D. (2010). Sequential and iterative architectures for distributed model predictive control of nonlinear process systems. *AIChE Journal*, 56, 2137–2149.

Liu, J., Muñoz de la Peña, D., and Christofides, P.D. (2009). Distributed model predictive control of nonlinear process systems. *AIChE Journal*, 55, 1171–1184.

Müller, M.A. and Allgöwer, F. (2014). Distributed economic MPC: a framework for cooperative control problems. In *Proceedings of the 19th World Congress of the International Federation of Automatic Control*, 1029–1034. Cape Town, South Africa.

Özgülşen, F., Adomaitis, R.A., and Çinar, A. (1992). A numerical method for determining optimal parameter values in forced periodic operation. *Chemical Engineering Science*, 47, 605–613.

Qin, S.J. and Badgwell, T.A. (2003). A survey of industrial model predictive control technology. *Control Engineering Practice*, 11, 733–764.

Scattolini, R. (2009). Architectures for distributed and hierarchical model predictive control – A review. *Journal of Process Control*, 19, 723–731.

Wächter, A. and Biegler, L.T. (2006). On the implementation of an interior-point filter line-search algorithm for large-scale nonlinear programming. *Mathematical Programming*, 106, 25–57.